Grain Deformation and Strain in Board Level SnAgCu Solder Interconnects Under Deep Thermal Cycling

Seungbae Park, Ramji Dhakal, Lawrence Lehman, and Eric J. Cotts

***Abstract*—Digital image correlation and cross polarizer, optical microscopy were used to quantify the deformation behavior under deep thermal cycling of near eutectic SnAgCu (SAC) solder in board level interconnects. Maps with sub micron spatial resolution of the strain levels and von Mises strain were produced for selected cross sections. Large spatial variations in the thermo mechanical response of the solder joints were observed and were correlated with Sn grain boundaries or intermetallic precipitates. Such observations are consistent with the anisotropic nature of the mechanical properties of Sn, and the differences in the mechanical responses of Sn and the intermetallic precipitates in SAC solder. The demonstrated anisotropic thermomechanical response of many SAC solder joints sheds doubt on any model which considers these joints to be composed of isotropic material.**

***Index Terms*—Digital image correlation (DIC), fatigue life, grain boundary, intermetallics, SnAgCu (SAC), thermomechanical deformation.**

I. Introduction

RAPID progress is being made in the electronics industry towards a full manufacturing transition to Pb-free soldering technology. However, much of the established understanding of eutectic Pb-Sn solders does not pertain to near eutectic, SnAgCu (SAC), Pb-free solders. As would be expected, the constitutive relations developed for the mechanical response of eutectic Pb-Sn solder alloys do not apply to SAC solders. More daunting is the possibility that no such simple relation will accurately reflect the mechanical behavior of these new materials [1]–[3]. In any event, a better understanding of the mechanical response and failure mechanisms of SnAgCu solder joints is required for the construction of more realistic Pb-free solder assembly life models [1]–[3].

Board level, near eutectic SnAgCu ball grid array (BGA) interconnects, being primarily Sn-based solders, are generally observed to contain only one or a small number of Sn grains [4]–[8], in contrast to eutectic Pb-Sn solder joints, which contain micro scale regions of relatively soft Pb. Furthermore, these Sn grains are very often twinned, with twinning angles around the [010] axis near 60°. Thus, the orientations of these Sn grains are highly correlated [6]–[8]. This large grained Sn matrix contains Cu_6Sn_5 and Ag_3Sn intermetallic compound (IMC) precipitates. The size of these precipitates and the Sn grains depend on solder composition and reflow conditions. Primary Ag_3 Sn precipitates are often found to be shaped as needles or plates, while large Cu_6Sn_5 precipitates are generally rod like. The differences in the mechanical properties of Sn and these precipitates, and the inherent large anisotropies in both the mechanical properties and the CTE of Sn [7]–[9], mean that these Sn rich solders cannot generally be treated as homogeneous materials. In fact, in the thermal cycling experiments, fatigue cracks in lead-free solders are often observed propagating along the Sn grain boundaries, along the solder-pad interfaces [4], and also along the Sn/primary intermetallic interfaces [15].

To understand the thermo-mechanical response [9] of SAC solder joints and their failure mechanisms, better characterization and understanding of the evolution of the microstructure of these joints are required. This study employs a powerful combination of optical imaging techniques to examine the microstructure of SAC alloys. To characterize the size and distribution of IMCs, Sn grains and Sn grain boundaries, bright field (BF) and cross polarizer (XP) imaging techniques of optical microscopy have been used [Fig. 1(a) and (b)]. A relatively new technique, digital image correlation (DIC) [10]–[13], has been used to quantify accumulated plastic deformations and strains resulting from Thermal Cycling. These strain measurements are correlated with Sn grain boundaries and IMC locations in an attempt to better understand failure mechanisms in Pb free, SnAgCu solder joints. We find dramatic dependencies of the mechanical response of SAC solder joints on microstructure.

II. Experiment

A. Sample Preparation

A flip-chip plastic ball grid array (PBGA) package in a 20×20 array (CASTIN alloy: Sn-2.5Ag-0.8Cu-0.5Sb) and a flip chip ceramic ball grid array (CBGA) package in a 25×25 array (Sn-3.8 Ag-0.7 Cu) of lead-free board level interconnects in 1.27-mm pitch were each sectioned to obtain strips with four rows of solder balls. In the PBGA package, the copper pads on the substrate side had an electroless nickel immersion gold (ENIG) coating and the pads on the board side were bare copper with organic solderability preservative (OSP). In the CBGA package, on the substrate side were ceramic pads with

Manuscript received February 8, 2006; revised November 1, 2006. This work was supported in part by IEEC of SUNY Binghamton. This work was recommended for publication by Associate Editor A. Chandra upon evaluation of the reviewers' comments.

S. Park and R. Dhakal are with the Department of Mechanical Engineering, State University of New York at Binghamton, Binghamton, NY 13902 USA (e-mail: sbpark@binghamton.edu).

L. Lehman and E. J. Cotts are with the Physics Department, State University of New York at Binghamton, Binghamton, NY 13902 USA.

Color versions of one or more of the figures in this paper are available online at http://ieeexplore.ieee.org.

Digital Object Identifier 10.1109/TCAPT.2007.892101

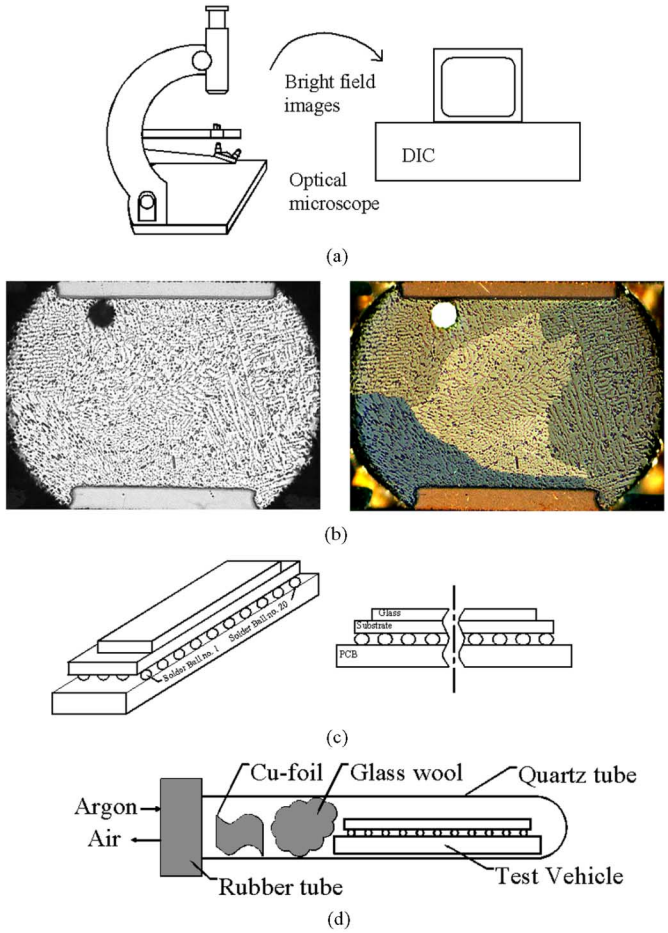

Fig. 1. Schematic of the experimental procedure and test sample showing the bright field and cross polarized images of a cross section of a 35 mil diameter PBGA solder ball showing variation of gray scale and different grains. The CBGA test vehicle had a ceramic substrate in place of glass and organic substrate: (a) a schematic of the expermental procedure, (b) image in bright field (left) and under a cross polarixer, (c) schematic of the PBGA package, and (d) schematic of the sealing setup.

a thin ENIG coating whereas the board side pads were copper with OSP. The first row in each strip of solder balls was ground and polished flat. Polishing was done manually, and without mounting, to avoid any mechanical effect of added epoxy on the solder balls. A relatively large mechanical fixture was used to hold the sample during polishing to ensure flatness of the cross-sectioned surface. The samples were ground flat using different grades of carbide papers and polishing was done with polishing cloths loaded with diamond pastes (6 μm to 1 μm) and polishing oil. It is important to maintain a flat cross section for digital image correlation. Also, to reveal the grain structures in the microscope images using a cross-polarizer, it is necessary to have the surface free from any polishing damage. The final polishing was done with 0.05-μm Alumina gel, followed by 0.02-μm silica gel for a very short duration, in order to expose the intermetallics. This surface consists of fine tin dendrites decorated with intermetallic precipitates. This provides a distinct variation of gray scale in the bright field images of the cross section, which is an important requirement of digital image correlation. The cross-sectioned solder ball numbering is shown in Fig. 1(c).

B. Setup

1) Digital Image Correlation (DIC): DIC is a full field optical measurement technique in which both the in-plane and out-of-plane deformations can be computed by comparing the pictures of a target object at initial and deformed stages [10]–[13]. It recognizes distinct features based on the gray scale variation in an image and assigns coordinates to these features. Local displacements or strains are determined from the movement of the features relative to their initial coordinates. In this process, thousands of unique correlation areas (known as facets) are defined across the entire imaging area. The center of each facet is a measurement point that can be thought of as an extensometer or strain rosette. These facet centers are tracked, in each successive pair of images, with accuracy of up to one thousandth of a pixel. Then, using the principles of photogrammetry, the coordinates of each facet are determined for each set of images. The results are the shape of the component, the displacements, and the strains. Rigid body motion can be quantified and removed to reveal local deformations.

For in-plane (2-D) DIC measurements, only one camera is required, using images before and after deformations. The challenges of 2-D DIC are generating the gray scale variation on the sample surface for image correlations and assuring surface flatness to maintain a good focus at all points on the measurement surface. In this study, the intermetallics present in the solder ball cross section were exposed by polishing with colloidal silica for a very short time; these clearly visible intermetallics were used as the irregular patterns required for DIC Fig. 1(b). Hence, the requirement of surface treatment for digital image correlation, which could be a tedious task for such a small-scale object [17], was naturally achieved.

2) Optical Microscopy: The combination of bright field and cross polarizer optical microscopy was used to delineate different Sn grains, and the location of Sn grain boundaries in the cross-sectioned samples. Since β-Sn is birefringent, cross polarizer microscopy reveals contrast between differently orientated Sn grains. For this technique to work well, it was important to have the final polished stage free from any polishing oriented defects. Such defects generally include recrystallization of the β-Sn phase, i.e., formation of a number of small Sn grains, which would obscure information on the Sn grain structure. Information on the locations of Sn grains grain boundaries as determined from cross polarizer, optical microscopy was correlated with the strain distribution in the Sn grains determined from DIC.

C. Procedure

The purpose of this analysis is to understand the deformation mechanism of SAC solder interconnects and thus to ultimately explain the failure mechanism associated with deep thermal cycling (DTC, -45 °C to 125 °C air to air). The XP images and strain/deformation information obtained from DIC can be used to better understand the role of grain boundaries, pad-solder interfaces and intermetallics in the cross section of solder interconnects on failure. It is hypothesized that the regions with maximum accumulated von Mises strain are sites with higher risk of crack initiation and propagation in the solder joints after further thermal cycles.

Bright field digital images of the interconnects were captured after final polishing as the reference images for DIC. Also, the images were taken under a cross polarizer in order to identify Sn grain boundaries [4], [5]. Subsequently, the sample was sealed in a quartz tube in an Argon environment with a Cu-getter to absorb remaining oxygen, and with glass wool to secure the Cu-foil in the tube. The sealing set up is shown in Fig. 1(d). The whole tube was subjected to deep thermal cycling in a convection air environmental chamber. A thermocouple was attached to the surface of the quartz tube to monitor the actual sample temperature during thermal cycling. The total duration of a cycle was 110 min, including a dwell of 10 min at the two peak temperatures. Because of the slower ramp rate and the dwelling time at the extremes, the sample is expected to have gone through the same temperature loading as shown by the thermocouple on the glass surface although quartz and argon are both relatively good insulators. After thermal cycling, the sample was removed from the quartz tube and images were again captured using both cross polarizer and bright field digital imaging microscopy. The bright field images, before and after thermal cycling, were used for image correlation to quantify the deformations and strains on the cross section; and compared with the locations of different grains and grain boundaries as discerned in the XP images.

III. Results and Analysis

Fig. 2 shows cross-polarized images of solder balls before stressing and after 100 DTCs. The large regions of one shade or color in a solder ball correspond to particular Sn grains [Fig. 2(a) and (b)]. In the case of the solder balls that appeared to be single-grained in the cross-sectioned plane (i.e., those of single shade or color) [Fig. 2(c) and (d)], new contrast was readily apparent at the pad-solder interfaces after 100 DTCs. A mottled area along the interface was observed. In the case of SAC solder joints with more than one Sn grain; such significant surface damage was also visible at grain boundaries Fig. 2(b), as well as along the solder-pad interfaces. This surface damage was identified as out-of-plane extrusions or intrusions of the solder. Samples were polished further to examine the extent of such damage throughout the solder ball thickness. It was found after removing only a few microns that the degree of damage was minimal, if observable.

We identify such surface damage with significant deformation in the given region. A significant amount of deformation observed near pad-solder interfaces after 100 DTC cycles is consistent with the general results of other long-term aging studies, which often report failure in this region [2]–[5]. Furthermore, the observation of significant deformation along grain boundaries is consistent with previous studies, which have concluded that grain boundary sliding is an important deformation mechanism at similar temperatures in these systems. The present in situ observations of SAC solder joints during deep thermal cycling appear to be quite sensitive to resulting deformation in the solder balls.

It is noted that the deformation after 100 DTC cycles at package/PCB pad interfaces is particularly increased in the case of single Sn grain solder balls [e.g., Fig. 2(d)], as compared to the sample with a number of Sn grains Fig. 2(b). Apparently the absence of Sn grain boundaries in the bulk of this solder joint, and thus the absence of grain boundary sliding mechanisms, resulted in higher stress concentrations at the interfaces. It has been previously observed that the amount of deformation of a particular region of Sn is dependent on the availability of slip planes in the section. It has also been reported that after

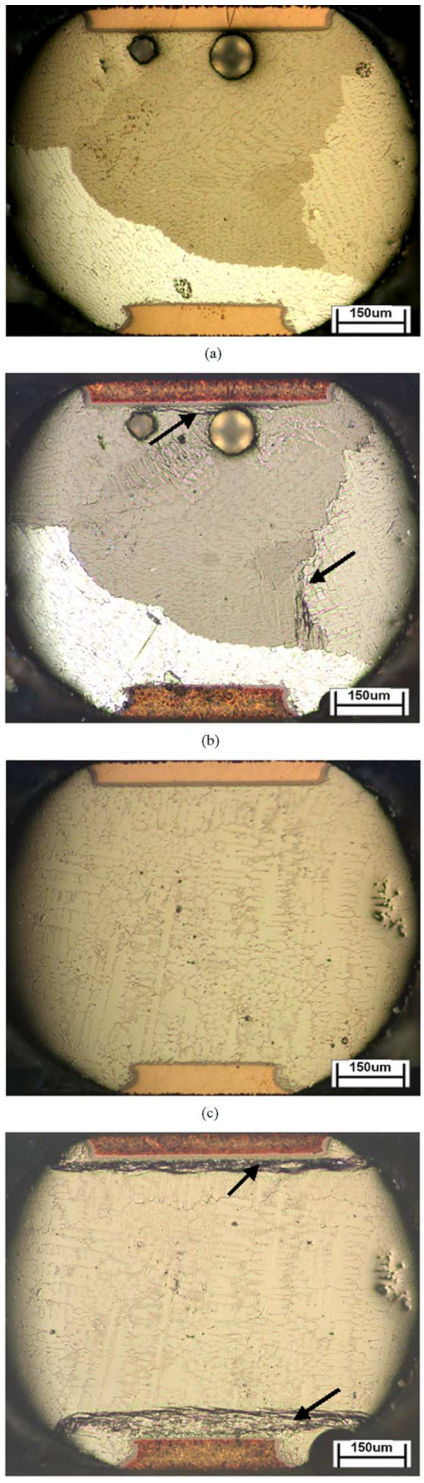

Fig. 2. XP images of PBGA solder balls before and after 100 cycles of DTC, −45 °C to 125 °C showing deformation along the grain boundaries and along the pad-solder interfaces: (a) XP image of Ball no. 3 before DTC, (b) XP image of Ball no. 3 aftr 100 cycles of DTC, (c) XP image of Ball no. 4 before DTC, and (d) XP image of Ball no. 4. after 100 cycles of DTC.

long-term aging, the pad-solder interface area becomes more brittle [4] and fails. The present observations indicate that the number of Sn grains can be important in determining the nature of deformation in the bulk of the SAC solder joint, and at the solder/pad interfaces.

DIC was used to determine the strain and plastic deformation accumulated in SAC solder joints after deep thermal cycling. The strain data are lost in some portions of the solder joints. Certain areas in a cross section, especially the solder/pad interfaces, could not be traced because of very large deformation in those regions. After such very large deformations, the gray scale in the images of those areas varies too much as compared to that in the undeformed images. Another general observation was that DIC showed a distinct variation in the strain distribution from solder joint to joint. This general variation can be attributed to the changes in the distance from neutral point (DNP) of the joints, though some variation can be attributed to the difference in Sn grain orientations from solder joint to solder joint. In this study we focus on the effect of Sn grain size, number and orientation on the mechanical response of each particular SAC solder joint.

Accumulated plastic deformations and strains in one particular SAC solder joint quantified by DIC are shown in Fig. 3(c) and (d). A black line is superimposed on these contour plots to represent selected Sn grain boundaries, whose location was determined by XP optical microscopy Fig. 3(b). The correlation between the region of highest strain and this particular grain boundary is evident. Vertical deformations of the grains above and below the black line are distinctly different. It is reasonable to expect uniform distribution of vertical displacement if the material is homogenous. However, the deformation is observed to be uniform only within each Sn grain.

Determinations of von Mises strain, which reflects the mixed strain status of a material, was used to identify regions where cracks are more likely to initiate. The von Mises strain is the scalar combining six strain tensors and is related to the distortional energy, which has been found to lead to the failure of a material. Von Mises strain Fig. 3(d) gives a clear indication of maximum plastic strain distribution along the grain boundary. Thus, a crack would be expected to initiate at the top right hand side location of the grain boundary, where about 3% of von Mises strain is accumulated after 35 DTC cycles. Similar results are seen in Fig. 4(b) and (d) where the strain and deformation fields are different for different grains and there is a maximum plastic strain accumulation along a grain boundary.

The general indication is that the Sn grain size and orientation is very important in determining the failure mechanism of the SAC solder joints. It should be emphasized that Figs. 3, 4, and 6 represent cyclic twinned solder joints. These solder joints comprise multiple grains, but with highly correlated orientations. All the twin segments share a common [010] twin rotation axis. Each twin segment is rotated 60° with respect to its neighbor. So we know, in these cases, that the misorientation between grains is not small [5], [7]. This is consistent with the strain distribution and the concentration of von Mises strain in the region of these high angle grain boundaries.

It is observed that the number and orientation of Sn grains observed in a cross section of a SAC solder ball significantly affects the mechanical response of the SAC solder joint. Of course, this Sn grain distribution can vary as a function of depth in the sample, particularly in the case of samples with many Sn

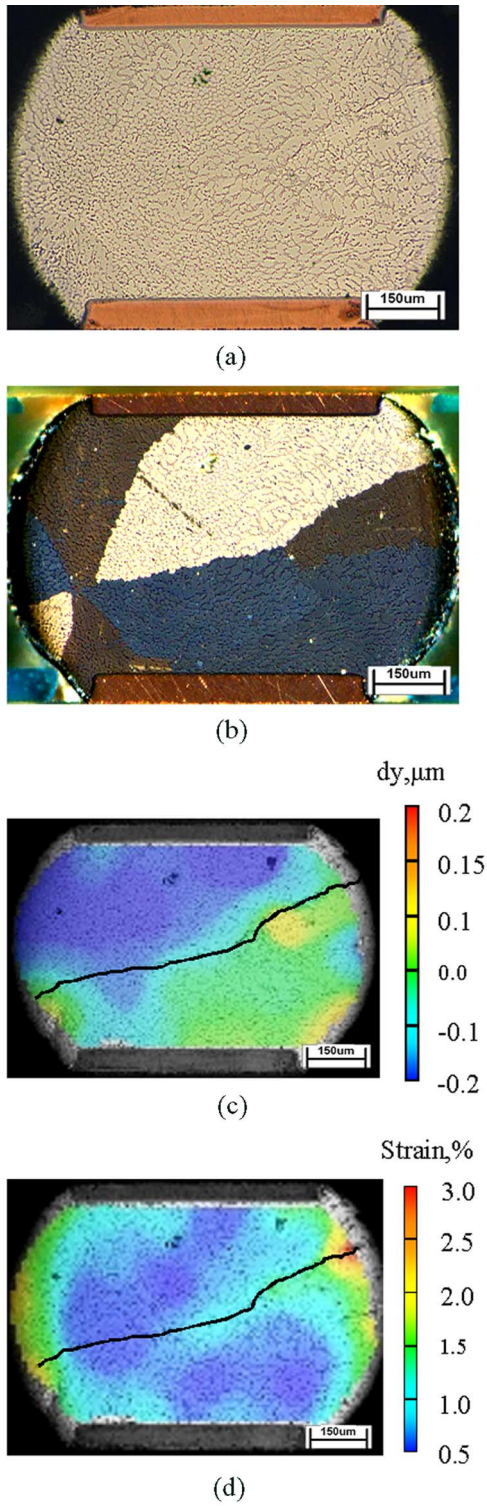

Fig. 3. Deformation and strain contour as obtained from DIC for PBGA Ball no. 3 after 35 cycles of DTC, (−45 °C to 125 °C). Image shows a cyclic twinned structure. The black lines show the location of some grain boundaries, (i.e., boundaries between twinned crystal segments): (a) BF image of Ball no. 3. before DTC, (b) XP image of Ball no. 3 before DTC, (c) Y-displacement of Ball no. 3 after 35 cycles of DTC, and (d) Von Mises stain of Ball no. 3 after 35 cycles of DTC.

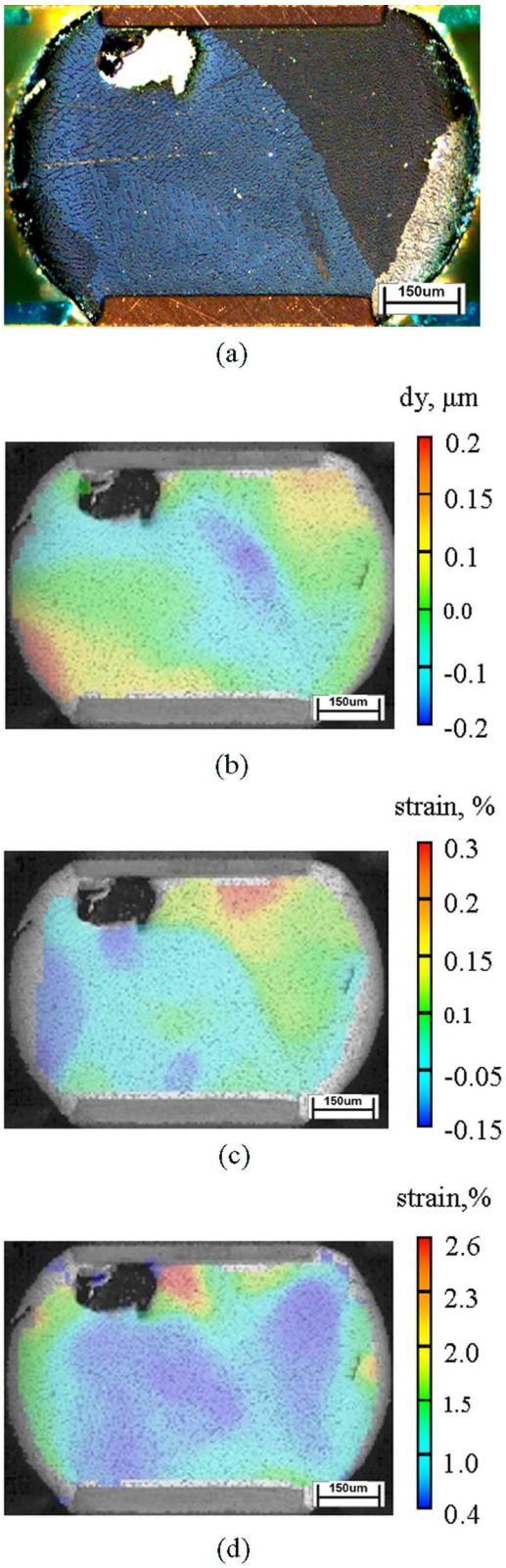

Fig. 4. XP image and Deformation and strain contour as obtained from DIC for PBGA Ball no. 5 after 35 cycles of DTC, (−45 °C to 125°C). (a) XP image of PBGA Ball no. 5 before DTC, (b) Y-displacement of PBGA Ball no. 5 after 35 cycles of DTC, (c) Y-strain of PBGA Ball no. 5 after 35 cycles of DTC, (d) Von Mises strain of PBGA Ball no. 5 after 35 cycles of DTC.

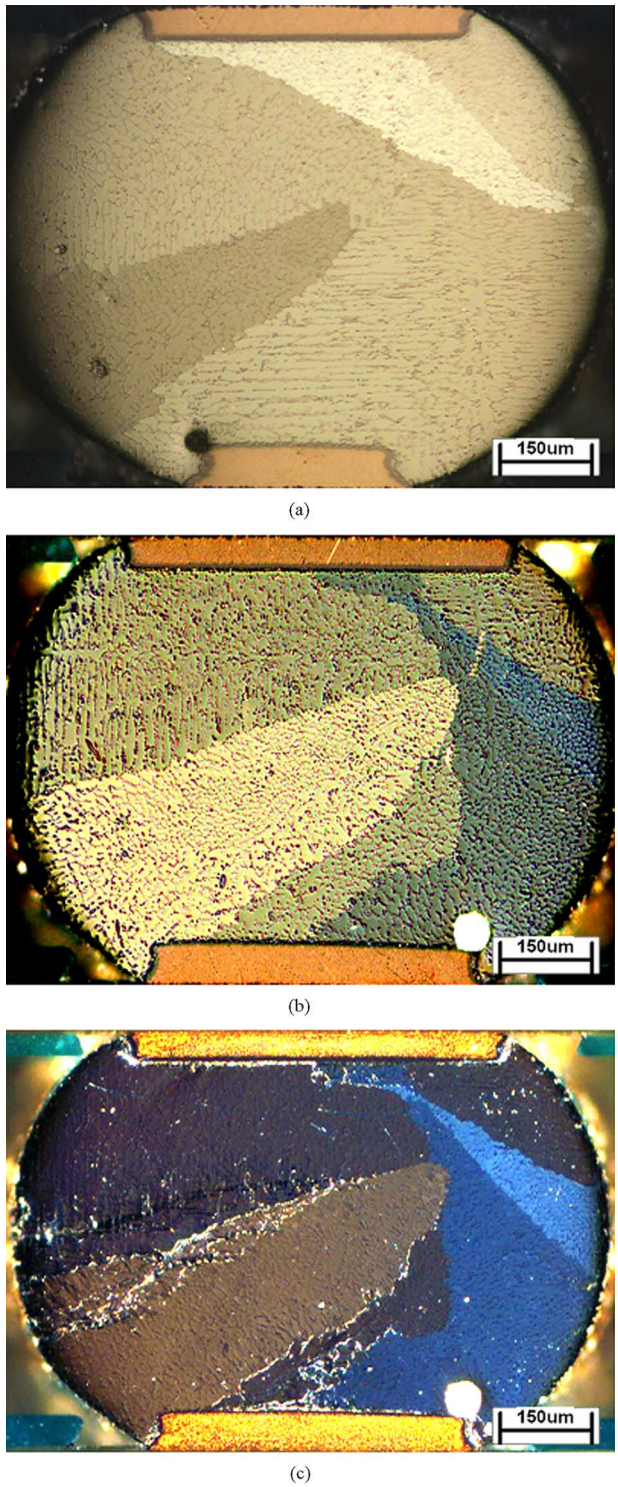

Fig. 5. Grain structures vary in different planes: images of solder ball No. 6 of PBGA at different sections after progressive polishing. The images show the 3-D nature of grains: (a) initial polished stage, (b) second polished stage, and (c) third polish after 400 cycles.

grains. Fig. 5 shows the grain distribution in a solder ball at different planes (through the depth) of a particular SAC solder ball, as revealed by repeated polishing of a cross-sectioned sample. The apparent diameter of the ball varies as the sample is further polished and the cross section approaches the mid plane of a solder ball. Only relative orientations of Sn grains on the cross-sectioned plane were measured, thus the colors of a particular Sn grain varied from figure to figure. One can see that the

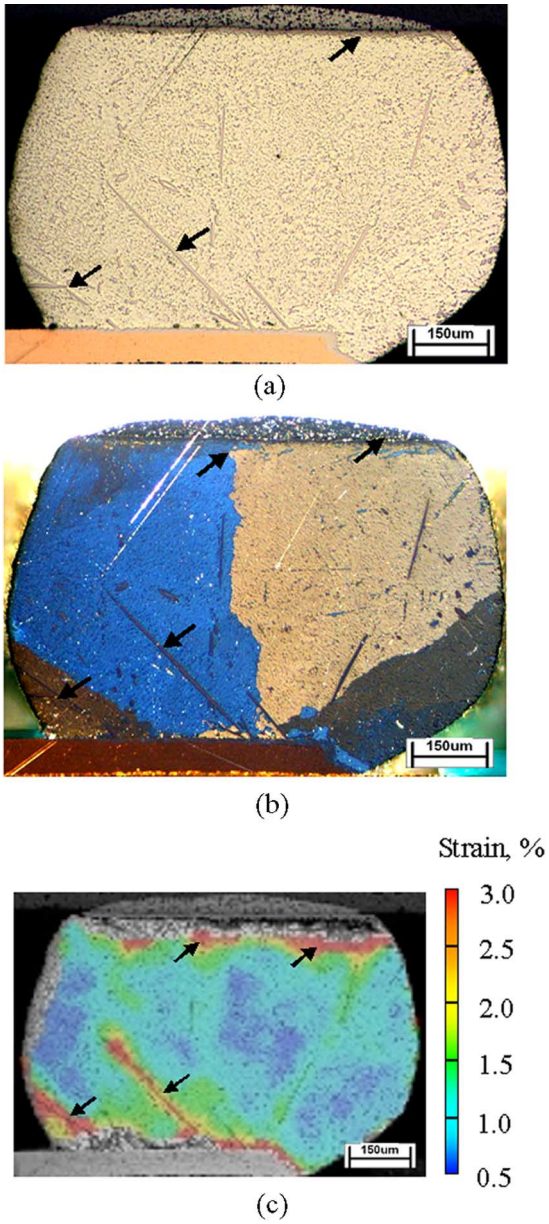

Fig. 6. Solder ball 19 of CBGA showing the BF image, XP image and DIC results of Von Mises strain superimposed on top of the BF image of the deformed ball after 22 cycles of DTC, (−45 °C to 125 °C). Arrows indicate the location of primary intermetallics of Ag_3Sn plates and grain boundary. This ball is also cyclic twinned, but the nucleation center was at the surface of the copper pad. Thus the grain boundaries are between twinned segments of the crystal: (a) BF image of CBGA Ball no. 19 before DTC, (b) XP image of CBGA Ball no. 19 before DTC, and (c) Von Mises strain of CBGA Ball no. 19 after 22 cycles of DTC.

Sn grain size varies with progressive grinding into the depth of the ball. This means that the Sn grains can be irregularly shaped in three dimensions and distributed throughout the ball. Hence, it may be difficult to understand completely the sliding of grain boundaries in SAC solder joints by a single plane cross section. In a polycrystal (such as that of Fig. 5), continuity must be maintained during deformation so that the boundaries between the deforming crystals remain intact. Sn crystals, however, have only a limited number of preferred active slip systems to accommodate strains [5], [7]. Each grain tries to deform homogenously in conformity with the deformation of the specimen as a whole. The constraints imposed by continuity may cause considerable differences in the deformation between neighboring grains and within each grain.

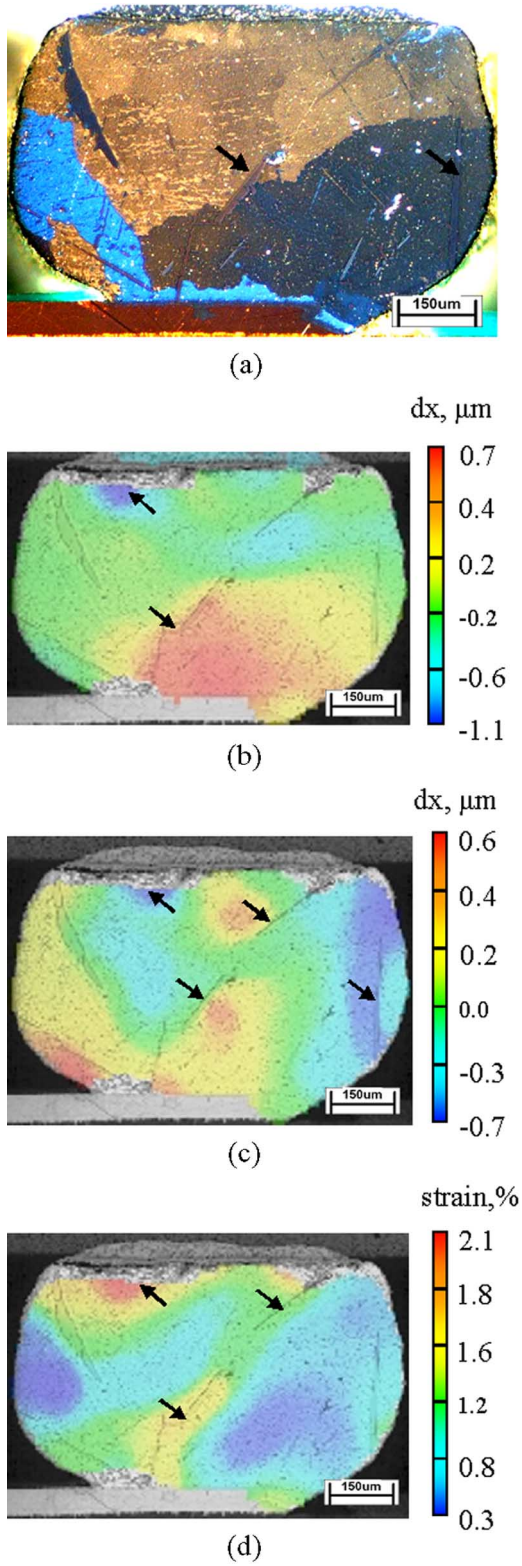

Fig. 7. XP image and Deformation and strain contour as obtained from DIC for CBGA Ball no. 8 after 22 cycles of DTC, (−45 °C to 125 °C): (a) XP image before DTC, (b) Y-displacement after 22 cycles of DTC, (c) Y-strain after 22 cycles of DTC, and (d) Von Mises strain after 22 cycles of DTC.

The present study provides some insight of the effect of IMCs on SAC solder ball deformation. This is particularly true because the PBGA solder balls had IMCs of distinctly different morphology than the CBGAs. The PBGA solder ball interconnects (Sn-2.5 Ag-0.8 Cu-0.5 Sb) had only very small IMCs, while the CBGA (Sn-3.8 Ag-0.7 Cu) exhibited primary intermetallics of long Ag_3Sn plates. This is consistent with previous studies of the effect of Ag content on IMC formation in near eutectic SAC alloys; SAC alloys with Ag concentrations below approximately 2.8 wt% form few if any Ag_3Sn plates under a normal range of cooling rates.

In the case of the CBGA assembly tested, the larger primary intermetallics of Ag_3Sn plates were observed to have a considerable effect on the deformation pattern of the solder ball (Figs. 6 and 7). Figs. 6(c) and 7(d) show a very high strain mismatch between some Ag_3Sn plates and the surrounding solder. A high von Mises strain accumulation is also observed along the pad solder interfaces. The locations of primary intermetallic precipitates, grain boundaries and pad-solder interfaces have been shown with arrows. The Ag_3Sn primary precipitate does have different thermomechanical characteristics, such as CTE and modulus, than the surrounding Sn. The CTE of Ag_3Sn is approximately $20\times10^{-6}/^{\circ}$C [14] though it is not known what anisotropy exists. Specifically, the large strain values near the Ag_3Sn plates Fig. 6(c) can be attributed to the resistance to deformation (stiffness) offered by the intermetallics, and the CTE mismatch between the bulk Sn and the primary intermetallics. Also, higher plastic strains are observed at the pad/solder interface area. The location and size of the plates are also important in an assessment of the effect of large plates on the reliability of solder joints since they provide an interphase interface where Sn grain sliding can occur during thermal loading. Because of the difference in strain fields near the IMCs and adjoining grains, the primary intermetallics can also be possible sites of crack initiation and propagation. It also depends on the size of the intermetallics and their location with respect to grain boundary and pad area [8]. The effects of primary intermetallics and different grain orientations observed in these tests are in accordance with the strain analyses performed on the same cross sections under In-situ thermal loading conditions [18]. *In-situ* tests provided a strong evidence of strain mismatches in different grain orientations and larger primary intermetallics [15], [16].

IV. Conclusion

A powerful combination of optical techniques was adopted to characterize the deformation and failure mechanisms of Pb-free near eutectic SAC BGA solder joints used in electronic packages. DIC was used to quantify the deformation and strain of different grains and IMCs by analyzing the bright field images obtained from the optical microscope before and after thermal loading. Crossed polarizer imaging was used to discern the grain orientations and to locate the positions of grain boundaries.

The effects of different grain orientations, grain boundaries and pad-solder interfaces on the strain distribution were explored. During DTC, near pad regions, especially in single grain balls, accumulate disproportionate levels of damage. In case of multi grain solder balls, some grain boundaries were found to accumulate disproportional damage. Strain is not uniformly distributed within the solder ball and is found to vary in the different grains and the IMC's. It was also observed that there is a higher strain field along some of the larger primary intermetallics of Ag_3Sn and the strain distribution is different from the different grains in the cross section. It is hoped that the further application of this technique will contribute towards building better reliability models of lead-free solders and ultimately increase the fatigue life of the packages with the optimized process conditions which tends to form different grain structures and intermetallic sizes.

Acknowledgment

The authors would like to thank L. Zavalij, Physics Department, SUNY Binghamton, for her guidance through different polishing stages of the sample preparation.

References

[1] X. Shi, H. L. J. Pang, X. R. Zhang, Q. J. Liu, and M. Ying, "*In-Situ* micro-digital image speckle correlation technique for characterization of materials' properties and verification of numerical models," *IEEE Trans. Compon. Packag. Technol.*, vol. 27, no. 4, pp. 659–667, Dec. 2004.

[2] A. Syed, "Accumulated creep strain and energy density based thermal fatigue life prediction models for SnAgCu solder joints," in *Proc. 54th Electron. Comp. Technol. Conf.*, 2004, vol. 1, pp. 737–746.

[3] R. Dudek, R. Doring, and B. Michel, "Reliability prediction of area array solder joints," *J. Electron. Packag.*, vol. 125, pp. 562–568, 2003.

[4] D. W. Henderson, "The microstructure of Sn in near eutectic Sn-Ag-Cu alloy solder joints and its role in thermomechanical fatigue," *J. Mater. Res.*, vol. 19, no. 6, pp. 1608–1612, 2004.

[5] L. P. Lehman, S. N. Athavale, T. Z. Fullem, A. C. Giamis, R. K. Kinyanjui, M. Lowenstein, K. Mather, R. Patel, D. Rae, J. Wang, Y. Xing, L. Zavalij, P. Borgesen, and E. J. Cotts, "Growth of Sn and intermetallic compounds in Sn-Ag-Cu solder," *J. Electron. Mater.*, vol. 33, no. 12, pp. 1429–1439, 2004.

[6] R. Kinyanjui, L. P. Lehman, L. Zavalij, and E. Cotts, "Effect of sample size on the solidification temperature and microstructure of SnAgCu near eutectic alloys," *J. Mater. Res.*, vol. 20, pp. 2914–, 2005.

[7] A. U. Telang, T. R. Bieler, J. P. Lucas, K. N. Subramanian, L. P. Lehman, Y. Xing, and E. J. Cotts, "Grain boundary character and grain growth in bulk Tin and Bulk lead-free solder alloys," *J. Electron. Mater.*, vol. 33, no. 12, pp. 1412–23, Dec. 2004.

[8] D. W. Henderson, T. Gosselin, and A. Sarkhel, "Ag_3Sn plate formation in the solidification of near ternary eutectic Sn-Ag-Cu alloys," *J. Mater. Res.*, vol. 17, no. 11, pp. 2775–2778, 2002.

[9] K. N. Subramanian and J. G. Lee, "Effect of anisotropy of tin on thermomechanical behavior of solder joints," *J. Mater. Sci.: Mater. Electron.*, vol. 15, pp. 235–240, 2004.

[10] M. A. Sutton, S. R. McNeill, J. D. Helm, and Y. J. Chao, "Advances in two-dimensional and three-dimensional computer vision," *Photomech., Topics Appl. Phys.*, vol. 77, pp. 323–372, 2000.

[11] P. C. Hung and A. S. Voloshin, "In-plane strain measurement by digital image correlation," *J. Braz. Soc. Mech. Sci. Eng.*, vol. 25, pp. 2215–, 2003.

[12] P. Cheng, M. A. Sutton, H. W. Schreier, and S. R. McNeill, "Full-field speckle pattern image correlation with B-spline deformation function," *Exper. Mech.*, vol. 42, no. 3, pp. 344–52, Sep. 2002.

[13] T. Schmidt, J. Tyson, and K. Galanulis, "Full-field dynamic displacement and strain measurement using advanced 3D image correlation photogrammetry," *Exper. Tech.*, vol. 27, no. 3, pt. I, pp. 47–50, May/Jun. 2003.

[14] S. Zarembo, L. Zavalij, and E. Cotts, Private Communication.

[15] K. S. Kim, S. H. Huh, and K. Suganuma, "Effects of intermetallics compounds on properties of Sn-Ag-Cu lead free solder joints," *J. Alloys Compounds*, vol. 352, pp. 226–236, 2003.

[16] S. Ahat, M. Sheng, and L. Luo, "Effects of static thermal aging and thermal cycling on the microstructure and shear strength of $Sn_{95.5}Ag_{3.8}Cu_{0.7}$ solder joints," *J. Mater. Res.*, vol. 16, no. 10, pp. 2914–2921, Oct. 2001.

[17] S. B. Park, R. Dhakal, and R. Joshi, "Comparative analysis of BGA deformations and strains using digital image correlation and Moiré interferometry," in *Proc. SEM Annu. Conf. Expo Exper. Appl. Mech.*, Portland, OR, Jun. 2005, [CD ROM].

[18] S. B. Park, R. Dhakal, L. P. Lehman, and E. J. Cotts, "Intergrain deformations and strains in board level lead-free SnAgCu solder interconnects under in-situ thermal loading conditions," *Acta Mater.*, to be published.

Seungbae Park received the Ph.D. degree from Purdue University, West Lafayette, IN, in 1994.

He began his professional career as a Development Engineer with IBM Microelectronics Division, Endicott, NY. Later, he was engaged in the reliability of IBM's corporate flip chip technology in both leaded and lead-free solders and high performance packaging. After seven years in IBM, he started his academic career at the State University of New York at Binghamton in 2002. He has more than 40 technical publications and holds 4 US patents. His research interest is physical reliability of microelectronics and MEMS packaging. His current projects include Pb-free solder reliability, material and packaging of MEMS and wafer level packages, experimental and numerical analysis of flexible electronics, and development of optomechanics for small scale systems.

Dr. Park served for several technical committees including member of JEDEC 14-1 Reliability Committee, co-chair of iNEMI Modeling and Simulation TWG, and chair of "Electronics Packaging" Council in the Society of Experimental Mechanics. He was a co-organizer of the 1st International Symposium on Optical Methodologies and Metrologies for Microelectronics and Photonics and the "Emerging Technology" track in ITHERM'06.

Ramji Dhakal received the B.Tech. degree in mechanical engineering from the Indiant Institute of Technology, Roorkee and the M.S. degree in mechanical engineering from the State University of New York at Binghamton where he is currently pursuing the Ph.D. degree.

His experience includes the use of various optical metrology tools to study the reliability of electronic and MEMS packages. Currently, he is working on experimental and numerical characterization of lead free solder reliability.

Lawrence Lehman received the Ph.D. degree in metallurgical engineering from the University of Notre Dame, South Bend, IN, in 1986.

He worked at Argonne National Laboratory Materials Science Division, for six years as a TEM Microscopist studying mechanical deformation in metals. Then, he worked for IBM for 16 years. At IBM, he created a materials laboratory for the Printer Division, Endicott, NY. Later, he moved to the Thermal and Mechanical Analysis and Test Group, Microelectronics Division, where he worked on many aspects of solder joining and packaging technology. In 2001, he joined the Research Foundation, State University of New York at Binghamton and continued to study lead-free solders, including the nucleation and growth of the Sn phase and the resulting microstructures and crystallography. He has published several papers on these subjects. He is currently the Laboratory Manager for the Small Scale Systems Integration and Packaging Center, SUNY Binghamton. He holds five Patents.

Dr. Lehman received 14 Awards involving packaging and joining technologies.

Eric J. Cotts received the Ph.D. degree in physics from the University of Illinois, Urbana.

He serves as Professor of Physics and Materials Science, and is the Department Chair at the State University of New York at Binghamton. His research interests lie in the study of transport phenomena at small length scales, with an emphasis on issues related to microelectronics.